

measured distances for flight data currently available to the author. However, additional test results for a wide variety of soils should be obtained before any general statements concerning the method are made.

### References

- <sup>1</sup> Bekker, M. G. and Janosi, Z., "Analysis of towed pneu-

matic tires moving on soft ground," Armed Services Technical Information Agency 256315(LL-62) (March 1960).

<sup>2</sup> "A soil value system for land locomotion mechanics," Department of the Army, Ordnance Tank-Automotive Command, Research & Development Div., Land Locomotion Research Branch Res. Rept. 5 (December 1958).

<sup>3</sup> Hanamoto, B., Liston, R. A., and Parker, C. B., "Terrain criteria in vehicle design," Land Locomotion Lab. Rept. 85 (June 1963).

MAY-JUNE 1966

J. AIRCRAFT

VOL. 3, NO. 3

## Torsional Oscillation of Helicopter Blades Due to Stall

NORMAN D. HAM\*

*Massachusetts Institute of Technology, Cambridge, Mass.*

AND

MAURICE I. YOUNG†

*The Boeing Company, Morton, Pa.*

The amplitude of single degree of freedom torsional oscillations of highly loaded helicopter rotor blades is shown to be dependent on the blade mean pitch angle and the reduced frequency of the oscillation by experiments conducted in the static thrust condition. The origin of this torsional motion is indicated by consideration of the experimental chordwise pressure variation on a model helicopter blade during the stable limit cycle oscillation that occurs in the static thrust condition. The relationships between this torsional motion and the effective damping in pitch in the presence of stall are determined. The implications of these results in the forward flight condition are discussed qualitatively and illustrated by reference to flight test records. A simple numerical method of approximating the boundary of stable pitching-torsional oscillations in forward flight is described and a sample calculation shows good correlation with flight test results. The design problem is discussed briefly, and several refinements of blade planform are suggested as a potential means of avoiding the asymptotic rise in control loadings which now occur with contemporary design practice.

### Nomenclature

$b$	= section semichord, ft
$k$	= section reduced frequency $\omega b/V$
$x$	= nondimensional blade spanwise station
$C_T$	= rotor thrust coefficient
$I$	= pitching moment of inertia
$\Delta M$	= moment change at stall, ft/lb/ft
$R$	= rotor radius, ft
$V$	= section translational velocity, fps
$\alpha$	= section angle of attack
$\alpha_0$	= section mean angle of attack
$\alpha$	= amplitude of periodic angle of attack change
$\Delta\alpha_D$	= angle by which dynamic stall lags static stall
$\mu$	= rotor advance ratio $V/\Omega R$
$\omega$	= section angular frequency, rad/sec
$\rho$	= air density, slugs/ft <sup>3</sup>
$\sigma$	= rotor solidity
$\theta$	= blade pitch angle
$\theta_0$	= mean blade pitch angle
$\hat{\theta}$	= amplitude of periodic blade pitch change
$\zeta$	= damping ratio
$\bar{\zeta}$	= potential flow aerodynamic damping ratio
$\Omega$	= rotor rotational speed, rad/sec
$\Theta(x)$	= local fundamental torsion mode amplitude, rad

### Subscript

$\theta$  = rotor blade pitching motion

### Introduction

ONE of the factors that can limit improvements in helicopter forward flight performance is a sharp increase in rotor torsional loads and vibration levels as appreciable portions of the rotor blades become stalled on the retreating side of the disk. Such regions of blade stalling that occur frequently in forward flight are shown below.

A previous investigation<sup>1</sup> indicated that one possible origin of increased torsional loading of rotor blades due to stall encountered in forward flight was a sharp decrease in the aerodynamic damping in pitch of the blades as they stalled. Other investigations of harmonically oscillating wings in forced motion<sup>2-6</sup> demonstrated that under stalled conditions the average damping in pitch over a cycle can become substantially negative and is strongly dependent on the wing mean angle of attack, the reduced frequency of the harmonic motion, the oscillation amplitude, and the airfoil configuration. Reference 3 indicated that the origin of the negative damping was aerodynamic moment hysteresis. Reference 2 applied the results of Ref. 3 to show that for certain mean angles of attack, reduced frequencies, and amplitudes of oscillation, the mean damping in pitch was zero over a cycle, and that, under these conditions, a self-excited but self-limiting one degree of freedom limit cycle oscillation of prescribed amplitude could occur.

Such oscillating motion, sometimes called stall flutter, is encountered in the highly loaded axisymmetric flow conditions of rotating machinery such as aircraft propellers or gas

Received May 20, 1965; revision received January 19, 1966. Presented at the Symposium on the Noise and Loading Actions on Helicopters, V/STOL Aircraft, and Ground Effect Machines, The Institute of Sound and Vibration Research, The University, Southampton, England, September 1965. This research was sponsored in part by the U.S. Army Research Office, Durham, North Carolina.

\* Assistant Professor, Department of Aeronautics and Astronautics.

† Technology Manager, Advanced Technology, Vertol Division. Associate Fellow Member AIAA.

turbine compressors, but not in the relatively lightly loaded hovering helicopter rotor. However, in translational flight, local transient blade stalling can reduce the blade net damping in pitch to negative values. Only a few cycles of torsional motion are possible in practical rotor designs, before the blade becomes unstalled; the stable limit cycle motion of axisymmetric flow conditions therefore is not achieved usually. However, substantial increases in blade torsional stress and pitch link loads are possible by the combined effects of self-excitation and the response to external disturbances. For example, the blade bending-torsion coupling and center of pressure shifts due to reversed flow over the inner portion of the retreating blade can provide a triggering action. The in-plane and out-of-plane blade motions normally present also can contribute to crossing this unstable threshold.

### Limit Cycle Motion in the Static Thrust Condition

#### Experimental Procedure

The experimental equipment was essentially that of Ref. 1 with a modified blade root retention that minimized torsional friction by elimination of the needle bearing; and, it prevented torsional motion of the blade until it was released by remote control at which time a desired rotational speed was achieved. In addition to this, the mechanism permitted the application of a step torsional displacement of the blade when a substantial disturbance was required to induce limit cycle motion. One hinged blade with an independently hinged counterweight was used instead of the two-bladed rotor of Ref. 1. The present equipment is shown in Fig. 1.

All tests were performed in the static thrust condition. The rotor blade was set at the static pitch angle corresponding to the desired mean pitch angle at a given rotational speed. (This was necessary because of the twisting moment generated by rotation.) For cases in which violent torsional motion was likely to occur the blade was restrained from torsional freedom by the root retention device described previously. The rotor then was brought up to the desired rotational speed and the blade released. An oscillograph was used to record torsional oscillatory motion when it occurred. Other recorded signals were blade flapping motion and rotor rotational speed. This procedure was followed for rotational speeds of 10–50 rad/sec, using three different tension-torsion straps which have torsional stiffnesses of the ratio 1:3.4:8 for blade mean pitch settings from 10°–25°.

The effect of varying Reynolds numbers was investigated indirectly using masking tape with the forward edge cut in a saw tooth pattern to force boundary-layer transition at the 10% chord line of the blade. Preliminary tests of the static blade in a low turbulence wind tunnel indicated that at Reynolds numbers of 400,000 transition did not occur until the 50–60% chord point, unless transition was forced by application of masking tape in the manner described pre-

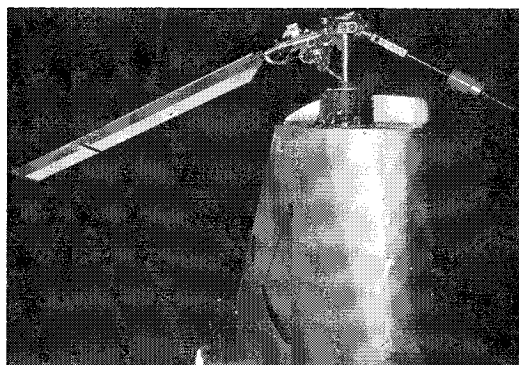


Fig. 1 Model rotor.

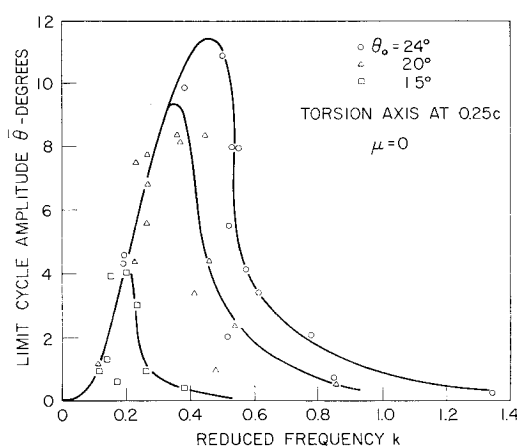


Fig. 2 Limit cycle amplitude vs reduced frequency.

viously. It was hoped that the early transition caused by the tape would approximate blade operation at supercritical Reynolds numbers of the order of 1,000,000.

The variation of aerodynamic moment during limit cycle motion was measured for the case  $\theta_0 = 20^\circ$ ,  $k = 0.35$  by means of eight pressure transducers located at 75% radius and the 10, 20, 30, 40, 50, 60, 70, and 80% chordwise stations. The pressure instrumentation is described in detail in Ref. 7.

#### Experimental Results

The experimental results are presented in terms of limit cycle half amplitude  $\bar{\theta}$  versus blade reduced frequency  $k = \omega_{\theta}b / 0.75\Omega R$  (i.e., based on rotational velocity at 75% radius), where  $\omega_{\theta}$  is the actual measured torsional frequency of the blade at the given rotational speed. The results are shown in Fig. 2 for various blade mean pitch settings  $\theta_0$ . The limit cycle amplitude was extremely sensitive to reduced frequency and pitch setting. Peak values occurred over a very narrow range of  $k$ ; elsewhere oscillatory amplitudes were virtually zero. The values of  $k$  corresponding to maximum limit cycle amplitude varied with the mean pitch setting.

The sensitivity to  $k$  is believed to be caused by the dynamics of boundary-layer separation. At low values of  $k$ , there is no lag in section moment change, i.e., the quarter chord moment at a given angle of attack is identical with that of the static case when the blade is at that angle of attack, and no destabilizing moments are generated. Then, at some critical value of  $k$ , moment changes occur after the static stall angle and generate an unstable hysteresis loop. At still higher values of  $k$ , virtually no further lag in moment change occurs and stabilizing effects become predominant. The sensitivity to  $\theta_0$  is related to the fact that at higher values of  $\theta_0$  the blade angle of attack is well above the stalling angle, and the increased lag in moment change associated with stall can generate larger amplitudes of blade pitching moment.

The effect of varying blade root torsional stiffness and varying rotor rotational speed was accounted for satisfactorily through use of the parameter  $k$  at the low Mach number of the present tests. Results for limit cycle amplitude for various torsional stiffnesses and rotational speeds "collapsed" when plotted against  $k$ . These results suggest that useful design information on stall aeroelastic effects for a rotor in forward flight can be deduced from hovering data if reduced frequency is based on the actual velocity at the reference radius of the retreating blade rather than on the mean velocity, i.e.,

$$k_{eff} = \omega_{\theta}b / \Omega R(x + \mu \sin \psi)$$

Reynolds number effects were not observed over the limited speed range of the rotating blade tests. Results for the clean blade and the blade with forced transition at the 10% position virtually were identical in all cases investigated. This may be due to the blade wake from preceding revolu-

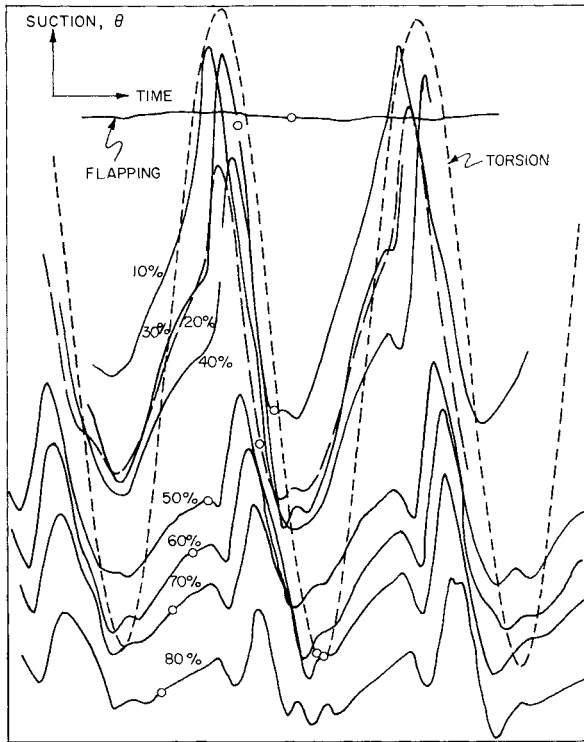


Fig. 3 Pressure data.

tions having caused sufficient turbulence to assure that the blade boundary layer was always turbulent. Another possibility is that the centrifugal effects associated with rotation stabilized the boundary layer to the extent that the transition caused by the application of masking tape in the static blade tests described previously now no longer existed. Sufficient variation of Reynolds number by variation of rotor rotational speed was not possible in the present tests because of constraints imposed by model design and test procedure.

Chordwise pressure measurements at the 75% spanwise station for the case  $\theta_0 = 20^\circ$ ,  $k = 0.35$  are shown in Fig. 3. The corresponding moment and torsional motion variation are shown in Fig. 4. The large suction peak over the whole section after maximum positive torsional deflection causes a nose-down moment that is in phase with pitching velocity and adds energy to the motion. This suction peak apparently is caused by the shedding of very concentrated positive vorticity associated with the large change in lift when dynamic stalling occurs. The shed wake during stall flutter apparently is punctuated by this sharp concentration of vorticity, with an intermediate continuous variation of much lower intensity. The large suction peak produces the unstable hysteresis loop in the moment variation with pitch angle shown in Fig. 5, crossplotted from Fig. 4.

### Theoretical Discussion

This section contains the development of an elementary theoretical expression for the pitch damping of a two-dimensional wing in the presence of stall. The theory is based on

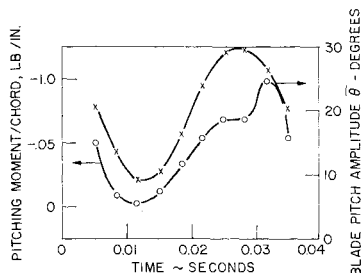


Fig. 4 Pitching moment, pitching amplitude time, histories.

the assumption that the reduction of effective pitch damping is due to aerodynamic moment hysteresis.

Consider the idealized symmetrical airfoil section static moment variation with angle of attack shown in Fig. 6. During pitching motion of a given amplitude the moment variation will include dynamic effects associated with the motion. For simple harmonic motion about the quarter chord below the stall, the additional moment will be that caused by potential flow damping,

$$C_1 \dot{\alpha} = \pi \rho b^3 V \dot{\alpha}$$

As shown in Ref. 3, this incremental moment variation is an ellipse superimposed on the static moment curve. Strictly speaking, the major axis of the ellipse should be inclined slightly with respect to the static moment curve in Fig. 6. Neglect of this inclination does not affect the following development.

Another dynamic effect associated with pitching motion is the time lag that occurs before the quarter chord moment decreases abruptly after the static stall angle is exceeded. Corresponding to this time lag is the lag angle  $2\Delta\alpha_D$  shown in Fig. 6. This lag angle is the source of aerodynamic moment hysteresis.

The total pitching moment variation through the stall then will follow the path of the arrow in Fig. 6 for total pitching amplitude  $2\bar{\alpha}$ . The area enclosed by the clockwise hysteresis loop represents energy added to the motion. This energy caused by moment hysteresis is, therefore, destabilizing. It is possible to determine an equivalent linear damping coefficient  $C_2$  by equating the energy required by one cycle of an equivalent viscous damper to the area of the hysteresis loop:

$$\pi C_2 \omega \bar{\alpha}^2 = \Delta M \cdot 2\Delta\alpha_D$$

Note that the additional area included by extending the hysteresis boundaries to the static moment curve will be cancelled exactly by the area created by considering the non-circulatory damping to exist over the entire cycle.

Therefore,

$$C_2 = (2/\pi\omega\bar{\alpha}^2) \Delta M \cdot \Delta\alpha_D$$

The total damping moment coefficient is

$$C = \pi \rho b^2 V - (2/\pi\omega\bar{\alpha}^2) \Delta M \cdot \Delta\alpha_D$$

$$C = I\omega[(\pi \rho b^4/I) \cdot (1/k)][1 - (2/\pi)^2(\Delta C_M \cdot \Delta\alpha_D/k\bar{\alpha}^2)]$$

since

$$\Delta C_M = (\Delta M/2\rho b^2 V^2)$$

$$k = (\omega b/V)$$

Now consider the pitching motion equation:

$$I\ddot{\alpha} + C\dot{\alpha} + I\omega^2\alpha = 0$$

The equivalent damping ratio is

$$\zeta = C/2I\omega = (\pi \rho b^4/2I) \cdot (1/k)[1 - (2/\pi)^2(\Delta C_M \cdot \Delta\alpha_D/k\bar{\alpha}^2)]$$

Limit cycle motion occurs when  $\zeta = 0$ . Therefore, solving for  $\bar{\alpha}^2$ ,

$$\bar{\alpha}^2 = (2/\pi)^2(\Delta C_M \cdot \Delta\alpha_D/k)$$

where  $\Delta\alpha_D$  is, in general, a function of  $\bar{\alpha}$ ,  $\alpha_0$ ,  $k$ .

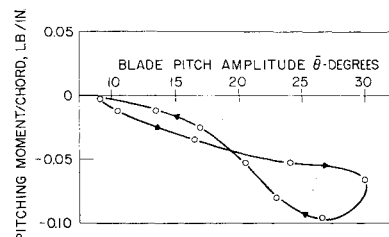


Fig. 5 Pitching moment vs pitching amplitude.

### Equivalent Damping in Pitch

In the previous section, the following expression was derived for blade pitch damping in the presence of stall:

$$\begin{aligned}\zeta/\bar{\zeta} &= \delta - (2/\pi)^2 (\Delta C_M/k\bar{\alpha}) \cdot \Delta\alpha_D/\bar{\alpha} \\ &= \delta - F(k, \alpha_0, RN, \text{airfoil}) 1/\bar{\alpha} \cdot \Delta\alpha_D/\bar{\alpha}\end{aligned}$$

where

$$\bar{\zeta} = (\pi\rho b^4/2I)(1/k)$$

$\delta = 1$  for torsion axis at 25% chord and no mechanical damping

Assume  $\Delta\alpha_D/\bar{\alpha} = \frac{1}{2}[1 - \Delta\alpha_s/\bar{\alpha}]$  for  $k = 0.25$ , based on Fig. 43 of Ref. 3;  $\Delta\alpha_s = \alpha_{\text{static}} - \alpha_0$

For two different oscillation amplitudes  $\bar{\alpha}_1$  and  $\bar{\alpha}_2$ ,

$$\frac{\zeta_2/\bar{\zeta} - \delta}{\zeta_1/\bar{\zeta} - \delta} = \frac{\bar{\alpha}_1}{\bar{\alpha}_2} \frac{1 - (\Delta\alpha_s/\bar{\alpha}_2)}{1 - (\Delta\alpha_s/\bar{\alpha}_1)} = r(\bar{\alpha}_1, \bar{\alpha}_2) \quad (1)$$

Therefore

$$\zeta_2/\bar{\zeta} = r\zeta_1/\bar{\zeta} + \delta(1 - r)$$

At all points on a limit cycle curve of  $\bar{\alpha}$  vs  $k$  for given  $\alpha_0$ , airfoil section, and Reynolds number:

$$\zeta_1/\bar{\zeta} = 0$$

Then

$$\zeta_2/\bar{\zeta} = \delta(1 - r) \quad (2)$$

This relationship permits the derivation of the equivalent aerodynamic damping for any  $\bar{\alpha}$  for given  $\alpha_0$ ,  $k$ , airfoil configuration, and Reynolds number. Damping curves obtained in this manner from the limit cycle curves of Fig. 2 are shown in Fig. 7 for the particular case  $\bar{\theta} = 0.1$  rads, taking  $\bar{\alpha} = \bar{\theta}$ . Implied in the method is the assumption that  $\Delta M$  is identical for  $\bar{\alpha}_1$  and  $\bar{\alpha}_2$ . It is interesting to note that the possibility of simple direct measurement of  $\zeta/\bar{\zeta}$  for various  $\bar{\theta}$  exists since a family of limit cycle curves could be obtained for a given  $\theta_0$  by mechanical variation of the parameter  $\delta$ .

### Implications in Forward Flight

#### A Generalized Pitch Damping Function

In the foregoing part of this paper, we have seen that static aerodynamic considerations do not provide a correct basis for understanding or predicting the character of rotor blade torsional oscillations. Furthermore, the existence of the stable limit cycle pitching-torsional oscillations shows that the theoretical predictions of potential flow unsteady aerodynamics for airfoil section pitch damping are progressively less representative as initial angle of attack increases towards the static stalling angle. The existence of the stable limit

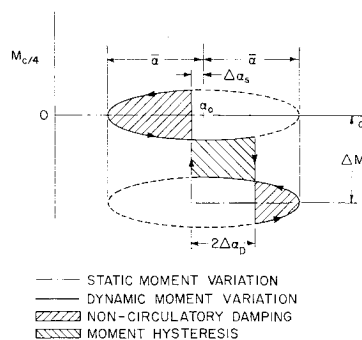
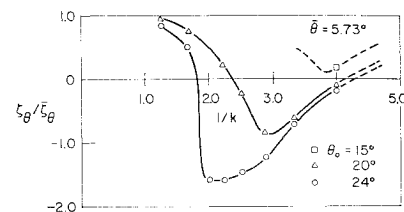


Fig. 6 Total pitching moment variation.

Fig. 7 Pitch damping deduced from limit cycle data.



cycle in high static thrust conditions demonstrates that, at critical combinations of initial angle of attack and reduced frequency of oscillation, the pitch damping is effectively negative. To provide a better appreciation of the possibilities and orders of magnitude of negative pitch damping, Fig. 8 was developed by a synthesis of data obtained by Ham, Rainey,<sup>4</sup> and Schnittger.<sup>2</sup> In the referenced experiments, the amplitudes of the stable limit cycle oscillation were developed as functions of the initial angle of attack and reduced frequency. In the synthesis of these data, an attempt was made to correct for experimental differences in rotation point and static stalling angles of the various airfoil sections. A straightforward calculation of equivalent viscous damping, based on the necessary balance of energy over a cycle of oscillation, yields a generalized equivalent viscous pitch damping function. Since this equivalent viscous damping function is obtained by an integrated averaging process, the higher frequency components of the destabilizing aerodynamic pitching moment are lost by smoothing. It is important therefore to note that the instantaneous values of negative damping that vary about this mean value can be substantially more negative near the stalling angle. This is to be expected by virtue of the strength of the previously mentioned vorticity, which would be shed at this juncture. The character of this generalized pitch damping function and the orders of magnitude of these mean values indicated in Fig. 8 have important implications for the helicopter in forward flight; significant regions of blade stall occur in many forward flight conditions.

#### Stall Flutter in Forward Flight

The extent of the stalled regions and the possibilities for unstable pitching-torsional oscillations are shown in Fig. 9, which illustrates the angle of attack distribution in a typical high speed cruise condition. There are two distributions shown. The first is based on the frequently made but arbitrary and untenable assumption of uniform induced velocity which suggests that there is a relatively small region of tip stall; the net integrated pitch damping over the blade is found to be positive in this case. In the second distribution, based on a more

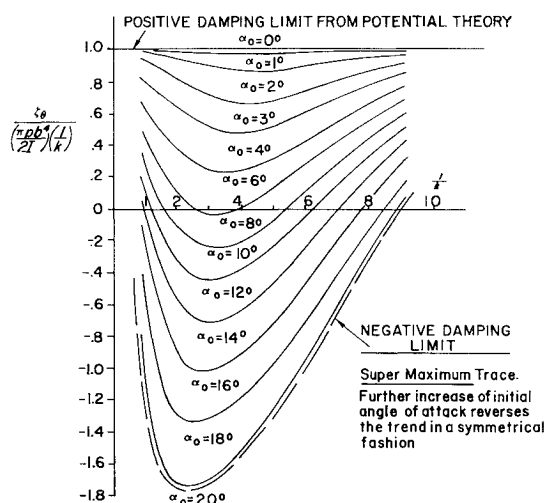


Fig. 8 Approximation for generalized pitch damping 0012 section quarter chord rotation point.

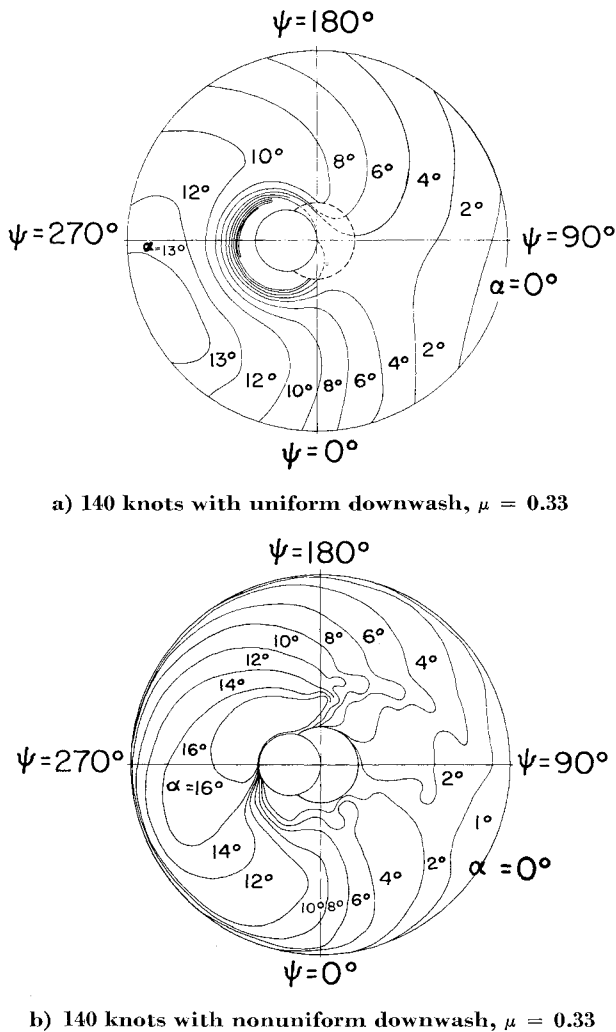


Fig. 9 Typical angle-of-attack distribution.

realistic vortex theory for calculation of the detailed rotor induced velocity field, an extensive region of stall is indicated; in this case, the net integrated pitch damping is found negative over a significant region of blade stations and azimuth angles. This indicates a strong likelihood of transiently unstable pitching-torsional oscillations; these would occur with a once per rotor revolution repetition rate.

Much experimental evidence of such pitching-torsional oscillations or rotor blade "stall flutter" is available. However, this has not been recognized heretofore as torsional instability of the rotor blade motion. The term "comfort stall" has been used in the past to describe an almost asymptotic rise in cyclic pitch link loadings and related helicopter vibratory phenomena that occur when significant zones of blade stall are present. Some typical experimental evidence

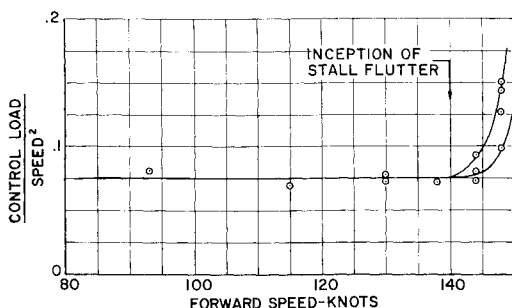


Fig. 10 Effect on control loads of the inception and growth of stall flutter.

of this asymptotic rise in cyclic pitch link loadings is presented in Fig. 10. A corresponding set of wave forms showing the detailed growth of the cyclic control loading as forward speed increases is presented in Fig. 11. A summary of these types of data presented in terms of limiting rotor loading conditions vs advance ratio is shown in Fig. 12, which is representative of the results of both flight testing and full scale rotor wind tunnel tests.

In view of the experimentally derived damping function, the current insight into the true rotor stall pattern, and this experimental evidence, there appears to be little doubt that the net pitch damping of the rotor blade can and often does become periodically negative in forward flight. There is also little doubt that many practical combinations of thrust coefficient-solidity ratio and rotor advance ratio result in significant zones of blade stall and an unstable torsional oscillation results.

#### Approximation for Stall Flutter Boundary

A simple method of prediction of rotor blade stall flutter appears possible. By analogy with classical flutter, we now indicate an analytic basis for the determination of stability limits or a flutter boundary. A more complicated calculation (not discussed here, but desirable in design) is an extension of the current methods for calculating the elastic blade response in bending and twisting, and an extension of such methods for the accompanying transmission of vibratory loads to the helicopter and to its rotating control system by accounting for the broad behavior of the damping in pitch. This is discussed briefly below.

The stability boundary can be approximated quite simply by considering the net aerodynamic pitch damping of the rotor blade and the control system's fundamental pitching-

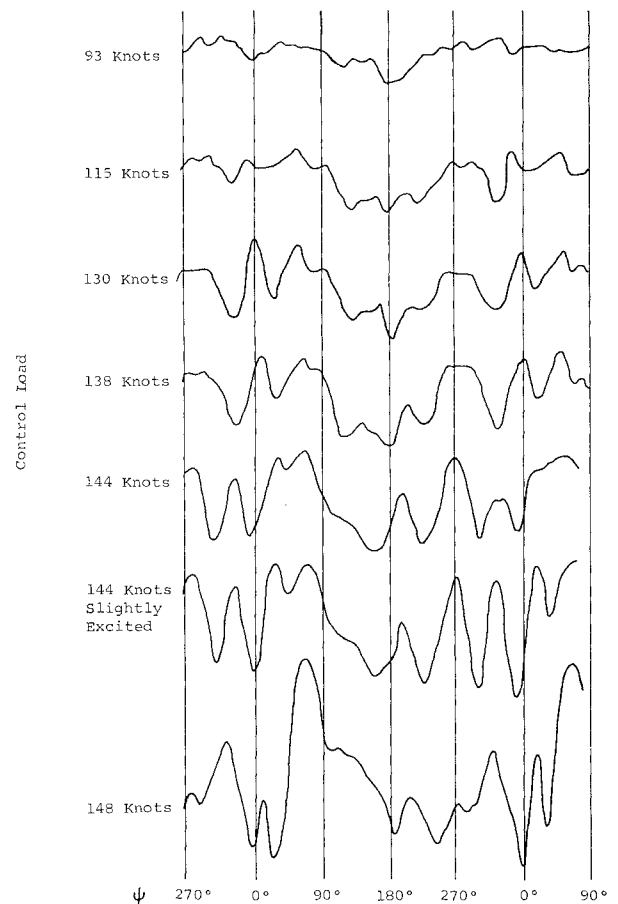


Fig. 11 Character of control load wave form with increasing speed.

torsional mode of oscillation. Because of the complex angle-of-attack distributions that are obtained in forward flight, this net damping function will vary widely with azimuth. Generally, it can be expected to exhibit a heavily damped condition in the region of blade advance, and a negatively damped condition in the region of blade retreat, whenever rotor thrust coefficient-solidity ratio and rotor advance ratio imply significant zones of stalling. Inasmuch as the instantaneous negative pitch damping can exceed the averages shown in Fig. 8, a simple approximation of the stability boundary is obtained by the condition that the motion will be transiently unstable if

$$[\zeta_\theta(\psi)]_{\text{weighted average}} \equiv \int_0^J \Theta_1^2(x) \zeta_\theta[\alpha_0(x, \psi), k(x, \psi), \times M(x, \psi), RN(x, \psi)] dx \leq 0 \quad (3)$$

In other words, the local blade element average damping ratio (depending on the local initial angle of attack and local reduced frequency) is weighted on an energy dissipation basis by the square of the local fundamental mode amplitude; this defines the net pitch damping of the rotor blade at each azimuth angle. If this weighted average damping becomes negative at any azimuth angle, the pitching-torsional motion can be expected to become transiently unstable. If the range of azimuth angles over which the pitch damping is negative is broad enough to permit one or more cycles of a pitching-torsional oscillation, a marked increase in cyclic control loading can be expected.

To illustrate the application of this stability criterion, a sample calculation of the net damping function vs azimuth angle was carried out for a relatively severe but practical rotor loading condition characterized by  $\mu = 0.17$  and  $C_T/\sigma = 0.111$ . The result of this calculation is presented in dimensional form in Fig. 13. It is seen that the net pitch damping is negative for the region bounded by the azimuth angles  $225^\circ$  and  $10^\circ$ . Stall flutter would be expected to occur. Figure 14 presents torsional strain and pressure data for this flight condition that support the theoretical prediction of stall flutter. The trace of absolute pressure transducer at the 80% radius station and the 5% chord point is indicative of the loss of leading edge suction and accompanying pitching moment variation. The blade torsional response to this initially nose-down moment exhibits an unstable behavior in the region in which the net damping in pitch is negative. In this case, the instability is short lived, but especially pronounced, as evidenced by the "spike" in the pitch link load trace near the  $330^\circ$  azimuth.

### Extended Methods of Rotor Analysis

The extension of current methods of rotor analysis to include the broad influence of transiently unstable blade pitching torsion oscillations is considerably more complex yet of great importance in design. It requires a more detailed

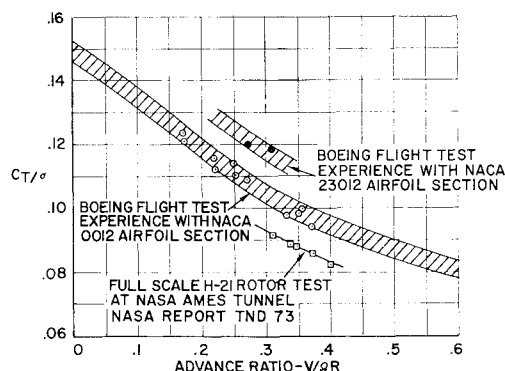


Fig. 12 Stall flutter limited rotor lift capability in forward flight based on full-scale wind tunnel and flight tests.

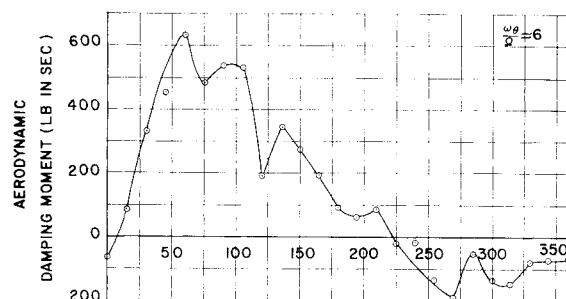


Fig. 13 Net aerodynamic damping moment for fundamental pitching torsion mode.

knowledge of the airfoil section pitching moment (as a function of both instantaneous angle to attack and rate of change of angle of attack) than is available at present. However, a first step in this direction has been made through consideration of the pressure variation along the airfoil during the experimentally induced stable limit cycle obtained in the static thrust condition.

Figure 3 is a sample of these data. It is quite evident that, as noted previously, the instantaneous pitching moment (and the negative damping) departs radically from the average over a cycle. If the sample pressure data were integrated to obtain the section pitching moment vs the instantaneous rate of change of angle of attack (strictly speaking vs pitch angle), the regions of positive and negative damping and the instantaneous values of damping coefficient needed for detail design could then be deduced. Experimental data of the type shown in Fig. 3 is believed to provide the basis for extending existing methods of rotor analysis to permit the detailed and reliable prediction of control load rise and general rotor characteristics beyond the stability boundary.

### Design Problem

Several approaches to rotor design which offer the possibility of avoiding rotor blade stall flutter suggest themselves. The first is to prevent significant regions of blade stall by increasing rotor solidity beyond that dictated by ordinary performance considerations. This approach, however, can result in an unacceptable performance penalty since excess solidity

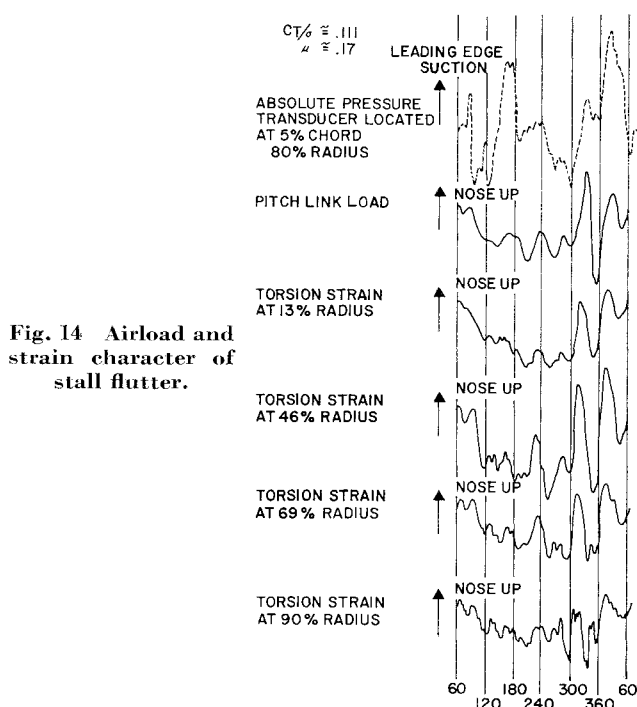


Fig. 14 Airload and strain character of stall flutter.

increases rotor profile drag and results in a reduced rotor lift to effective drag ratio at the design point, with the attendant loss in range and maximum speed capability. A second approach that is simple, but much less effective, is the attempt to offset the negative aerodynamic pitch damping with positive mechanical damping, since the deformation pattern associated with the fundamental pitching-torsion mode generally is dominated by twisting motion, with only a small amount of rigid body pitching against the effective torsional spring of the helicopter control system. In this case, a dashpot in parallel with the control system is relatively ineffective, leaving only internal torsional damping to offset the negative aerodynamic pitch damping; this is slight in conventional, monolithic metal rotor blade structures. A practical alternative is the use of a glass fiber resin matrix primary structure that could be expected to dissipate considerable energy in torsion; this is caused by internal (visco-elastic) damping, which varies with the rate of shear strain.

Perhaps the most appealing approach (with least performance penalty and design complication) is the reduction of the extent of the stalled zones by departure from the blade planform and twist distributions typical of contemporary design practice, where rotor blades have symmetrical airfoil sections, constant chord, linear twist, and the lifting portion of the blade commences at 15-20% of span. Approaches that appear promising for future high performance helicopters are those which utilize leading edge camber, reduce blade twist, and increase the root cutout relative to the contemporary design practice. Moderate planform taper also appears to have some value in this regard.

In summary, the combination of ample solidity, leading edge camber, reduced twist, increased root cutout, moderate planform taper, and a higher level of internal torsional damping appears to offer a practical means of avoiding rotor blade stall flutter in future high performance helicopters. Such a design should permit fuller utilization of the inherent rotor lift producing capability without the restrictive "comfort stall" boundaries that now prevail.

### Conclusions

The nature of stable limit cycle motion of a highly loaded helicopter rotor in the static thrust condition indicates that

the net aerodynamic damping of the torsional oscillations of a helicopter rotor blade becomes negative in the presence of stall for various combinations of mean angle of attack and local reduced frequency. The origin of the negative damping appears to be aerodynamic moment hysteresis resulting from the periodic shedding of intense vorticity at a blade angle of attack considerably above the nominal static stall angle.

The mean angles of attack and reduced frequencies characteristically encountered by the retreating blades of a helicopter in highly loaded forward flight conditions imply an extensive region of the rotor disk which would result in negative damping in pitch. Flight test and full scale wind tunnel records show substantial evidence of unstable torsional motion and excessive control loading consistent with theoretical prediction of negative torsional damping.

### References

- <sup>1</sup> Ham, N. D., "An experimental investigation of stall flutter," *J. Am. Helicopter Soc.* **7**, 3-16 (January 1962).
- <sup>2</sup> Schnittger, J. R., "Single degree of freedom flutter of compressor blades in separated flow," *J. Aeronaut. Sci.* **21**, 27-42 (January 1954).
- <sup>3</sup> Halfman, R. L., Johnson, H. C., and Haley, S. M., "Evaluation of high-angle-of-attack aerodynamic-derivative data and stall-flutter prediction techniques," NACA TN2533 (1951).
- <sup>4</sup> Rainey, A. G., "Preliminary study of some factors which affect the stall-flutter characteristics of thin wings," NACA Langley Aeronautical Lab., TN3622 (1956).
- <sup>5</sup> Rainey, A. G., "Measurement of aerodynamic forces for various mean angles of attack on an airfoil oscillating in pitch etc., with emphasis on damping in the stall," NACA Langley Aeronautical Lab., TR1305 (1957).
- <sup>6</sup> Bratt, J. B. and Wight, K. C., "The effect of mean incidence, amplitude of oscillation, profile and aspect ratio on pitching moment derivatives," *Aeronaut. Res. Comm R. and M.*, 2064 (1945).
- <sup>7</sup> Ham, N. D. and Madden, P. A., "An experimental investigation of rotor harmonic airloads including the effects of rotor-rotor interference and blade flexibility, U.S. Army AML TR 65-13 (1965).